



## Stability and dynamics of vacancy in graphene flakes: Edge effects

Adriano Santana<sup>a</sup>, Andrei M. Popov<sup>b</sup>, Elena Bichoutskaia<sup>a,\*</sup>

<sup>a</sup>School of Chemistry, University of Nottingham, University Park, Nottingham NG7 2RD, UK

<sup>b</sup>Institute for Spectroscopy, Russian Academy of Science, Fizicheskaya Str. 5, Troitsk, Moscow Reg. 142190, Russia

### ARTICLE INFO

#### Article history:

Received 9 October 2012

In final form 23 November 2012

Available online 1 December 2012

### ABSTRACT

Density functional theory calculations show that graphene flakes with monovacancy at the edge are energetically more stable than the flakes with vacancy in the middle. The energies of metastable and transition states for one step of vacancy motion towards the edge are calculated. We show that thermally activated motion of vacancy towards the edge occurs even at room temperature whereas the probability of return motion back to the middle is negligible. Molecular dynamics simulations of the vacancy motion in graphene flakes confirm this conclusion. The obtained results explain the mechanisms driving structural transformations in graphene.

© 2012 Elsevier B.V. All rights reserved.

### 1. Introduction

Experimental studies of the dynamics of individual carbon atoms in graphene have been empowered by the recent progress in aberration-corrected transmission electron microscopy (AC-TEM) capable of sub-Ångstrom resolution. The examples include AC-TEM observations of the formation and annealing of Stone–Wales defects [1], edge reconstruction [2,3] and formation of a large hole in graphene sheet from a single vacancy defect [3]. The AC-TEM has been also exploited in visualization in real time of the process of self-assembly of graphene nanoribbons from molecular precursors [4,5] and formation of nanometre size hollow protrusion on the nanotube sidewall [6]. Based on AC-TEM observations of transformation of small finite graphene flake into fullerene, a new ‘top-down’ mechanism for the formation of fullerene under the electron beam radiation has been proposed [7]. The critical step in the proposed ‘top-down’ mechanism of the fullerene formation is creation of vacancies in small graphene flake as a result of knock-on damage by electrons of the imaging electron beam (e-beam). The subsequent formation of pentagons at the vacancy sites near the edge reduces the number of dangling bonds and triggers the curving process of graphene flake into a closed fullerene structure [7]. Thus, dynamic behaviour of vacancies near graphene edge plays a crucial role in explaining mechanisms of the e-beam assisted self-assembly and structural transformations in graphene-like structures.

In a large (or infinite) graphene layer vacancy defects generated by the e-beam are stable at the time scale corresponding to *in situ* experimental conditions [8]. The formation and diffusion of vacancy defects in infinite graphene has been studied using a number

of computational methods [9–13]. The structure [14,15], energetics [15] and electronic properties [16] of hydrogenated graphene flakes with a single vacancy have been also discussed in the literature. The terminal hydrogen atoms are only weakly bound to a graphene flake, and due to considerably smaller atomic mass they can be easily removed from the edge by the e-beam at experimental imaging conditions suitable for visualization of structural transformations in graphene-like nanostructures. This letter presents the detailed study of the structure, energetics and dynamic behaviour of vacancy near the edge of non-terminated graphene flakes.

Our density functional theory (DFT) calculations show that stability of small flakes with monovacancy in the middle increases as the vacancy gets closer to the edge. The directional movement of a single vacancy in graphene has been previously shown only in relation to the edge reconstruction [2] and coalescence of vacancies into a vacancy cluster [12]. The transition state (TS) search performed in this work allows us to elucidate the TS geometry and the energy barriers for the motion of vacancy near the edge and to predict that the directional motion of vacancy towards the edge should occur even at room temperature. The characteristics of the directional motion of vacancy towards the edge of graphene flakes have been obtained from classical molecular dynamics (MD) simulations. We conclude that vacancies tend to migrate to the edge of small flakes even during such fast processes as the e-beam assisted self-assembly and structural transformation of graphene-like structures in AC-TEM. A possible mechanism for graphene self-healing is also discussed.

### 2. Methods

The structure and total energy of perfect flakes and flakes with vacancies have been calculated at the unrestricted Kohn–Sham [17], 6-31G<sup>+</sup>/B3LYP [18] level of theory as implemented in Q-Chem

\* Corresponding author.

E-mail address: [elena.bichoutskaia@nottingham.ac.uk](mailto:elena.bichoutskaia@nottingham.ac.uk) (E. Bichoutskaia).

quantum chemistry package [19]. The location of vacancy in graphene flakes with respect to the edge has a profound effect on its structure [20], so that the stable structure of monovacancy adopt either a 5/9- or a spiro-configuration. A 5/9 structure is generated by formation of an elongated carbon bond across the vacancy hole leading to creation of 5- and 9-membered ring. The 5/9 vacancy structure has radical character, and it is magnetic as it contributes an intrinsic magnetic moment of about  $1 \mu_B$  [21,22]. The spiro vacancy structure, on the other hand, does not contribute any unpaired electrons, and its structure differs significantly from the conventionally known 5/9 structure. The spin multiplicity of the metastable and transition states of small flakes with vacancy varies depending upon the size and symmetry of the flake. In all considered structures, the lowest energy states are found to be triplets. Vibrational frequency analysis has been carried out on the fully optimised structures to confirm the obtained metastable and transition states.

To study the dynamic behaviour of vacancies in graphene flakes canonical ensemble molecular dynamics (MD) simulations have been performed using GULP 3.1 software [23]. The carbon-carbon interactions are described using the Brenner potential [24]. The duration of each simulation run is 2 ns with 5 ps equilibration

time. At room temperature, the rate of processes leading to bond rearrangements in carbon network is too low, which makes their simulation prohibitive to MD technique. To overcome this problem the elevated temperatures are commonly used in MD simulations, and we perform MD simulations at 2500 K. At 2500 K, vacancy moves readily from the middle to the edge of the considered flakes and infinite graphene nanoribbons. Yet this simulation temperature is less than that of 2700 K required for the direct transformation of graphene flake into a bowl-shaped structure at tens ns time scale [25].

The model  $C_{116}$  flake has been studied using both DFT and MD approaches thus allowing a direct comparison of the results obtained with *ab initio* and classical force-field techniques.  $C_{116}$  is the biggest flake studied using DFT, and the full set of the optimised structures obtained with DFT comprises  $C_{52}$ ,  $C_{69}$ ,  $C_{88}$ ,  $C_{103}$  and  $C_{116}$  flakes, which are presented in Figure 1. A set of bigger graphene flakes,  $C_{116}$ ,  $C_{176}$ ,  $C_{248}$  and  $C_{332}$ , and short rectangular flakes,  $C_{395}$ ,  $C_{447}$ ,  $C_{623}$ , with vacancy in the middle studied in MD simulations is shown in Figure 2. Additionally, the dynamic behaviour of vacancy in an infinite zigzag graphene nanoribbon with 22 rows of atoms in width has been studied in periodic boundary conditions. The width of the infinite ribbon was therefore kept the

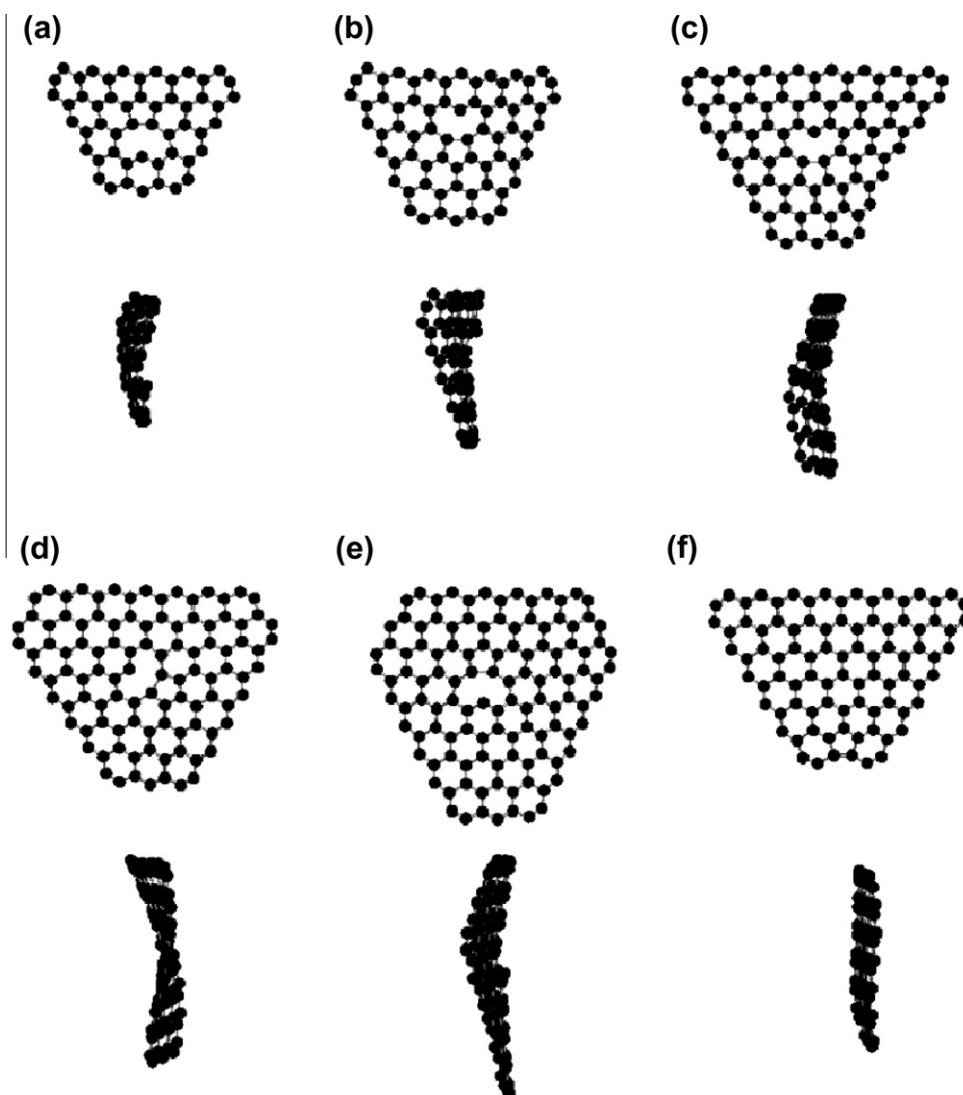


**Figure 1.** (a–e) The optimised structures of flakes with vacancy in the middle: (a)  $C_{52}$ , (b)  $C_{69}$ , (c)  $C_{88}$ , (d)  $C_{103}$ , (e)  $C_{116}$  and (f) the optimised structure of the  $C_{88}$  flake with vacancy at the edge. The side view corresponds to the flakes rotated by 90 degrees about the vertical axis in plane of the flake.

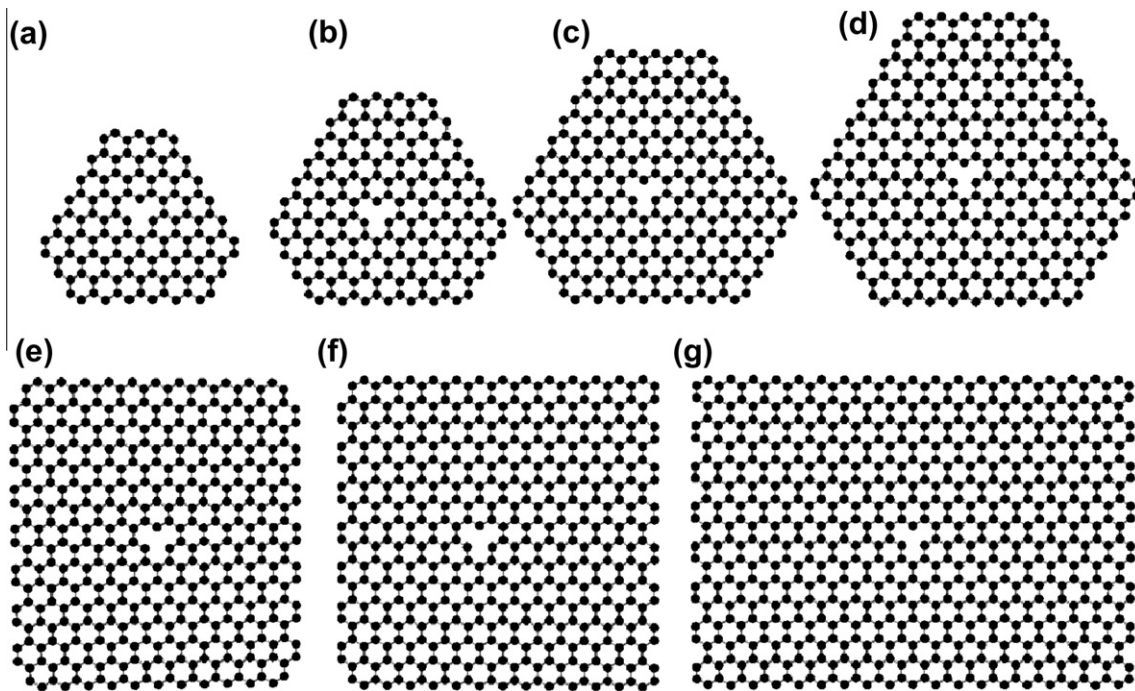


**Figure 2.** The initial structure of flakes with vacancy in the middle used in MD simulations; (a–d) hexagonal flakes with zigzag edges: (a) C<sub>116</sub>, (b) C<sub>176</sub>, (c) C<sub>248</sub>, (d) C<sub>332</sub>; (e–g) rectangular flakes with zigzag and armchair edges: (e) C<sub>395</sub>, (f) C<sub>447</sub>, (g) C<sub>623</sub>.

same the distance between zigzag edges of rectangular flakes shown in Figure 2e–g.

### 3. Results and discussion

In agreement with previous DFT calculations for hydrogen terminated graphene flakes [9,14] and infinite graphene layer [10], we obtain that a vacancy in the middle of graphene flake undergoes a Jahn–Teller distortion. This results in a well known 5/9 vacancy structure with two dangling bonds forming a weak reconstructed bond and a displacement of the remaining dangling carbon atom out of graphene plane. In the optimised structure of the C<sub>116</sub> flake shown in Figure 1e, the length of the weak reconstructed bond at a vacancy site is calculated to be 1.67 Å. This value is naturally smaller than those of  $2.1 \pm 0.1$  Å calculated for a flat undistorted flake [9] and 2.0 Å for infinite graphene [26]. The discrepancy stems from a considerable bending of the entire flake due to the formation of the 5/9 vacancy structure. These distortions of the optimised structure become most prominent as the flake gets smaller (see Figure 1). The edge vacancy, created by removal of carbon atom from zigzag edge of a flake, form a pentagon with a strong reconstructed bond of about 1.42 Å in length. No dangling bonds are present in the optimised structure of the edge vacancy, and flakes bend only slightly, mainly around the formed pentagon as shown in Figure 1f for the C<sub>88</sub> flake. In finite small graphene flakes structure deformation is not localised near the defect but affects the entire system. The thermodynamic stability of a defect in the distorted structure is higher than that in the undistorted flat structure.

The stability of flakes with vacancy in different locations with respect to the edge can be assessed by the cohesive energy per carbon atom,  $\mu_c$  defined as [4]

$$\mu_c = \frac{E^{\text{tot}} - nE_C}{n}, \quad (1)$$

where  $E^{\text{tot}}$  and  $E_C$  are the total energies of the flake and carbon atom, respectively, and  $n$  is the number of carbon atoms in the flake. The

calculated values for the cohesive energy of perfect flakes and the same flakes with a vacancy in the position shown in Figure 1a–e are given in Table 1. This table also contains DFT data for the formation energy of a vacancy in the middle,  $E_f$ , calculated as [13]

$$E_f = E_v^{\text{tot}} - E_p^{\text{tot}} \left( \frac{n_p - 1}{n_p} \right), \quad (2)$$

where  $E_p^{\text{tot}}$  and  $E_v^{\text{tot}}$  are the total energies of perfect flake and flake with vacancy, respectively, and  $n_p$  is the number of carbon atoms in the perfect flake. The obtained values of  $E_f$  are in the range of 6.8–8.0 eV in a good agreement with the experimental value of 7 eV [27] and previous theoretical calculations giving the values of 7.85 eV [13], 7.63 eV [28], 7.6/7.7 eV [26] for a vacancy in infinite graphene as well as that of 7.4 eV for a vacancy in the middle of the C<sub>120</sub>H<sub>27</sub> flake [9]. To study the energetic characteristics related to the motion of vacancy near graphene edge we compare the total energies of flakes with a vacancy in the middle and at the edge, and the calculated differences,  $\Delta E$ , between the total energies are presented in Table 1. The location of vacancy in the middle is shown in Figure 1a–e for all studied flakes, and an example of the edge vacancy structure is shown in Figure 1f for the C<sub>88</sub> flake. A considerable difference of  $\Delta E = 6.6$ –8.9 eV in the total energies has been found for all flakes.

The relative instability of vacancy in the middle of a small graphene flake is caused by the presence of dangling bond at va-

**Table 1**

The DFT energy characteristics of perfect flakes and flakes with vacancy located at distance  $d$  (in Å) from the edge:  $\mu_c$  (in eV) is the cohesive energy per carbon atom,  $E_f$  (in eV) is the energy of vacancy formation, and  $\Delta E$  (in eV) is the difference in the total energy of flake with vacancy in the middle and at the edge.

Perfect flake	$\mu_c$	Flake with vacancy	$\mu_c$	$E_f$	$\Delta E$	$d$
C <sub>53</sub>	−6.46	C <sub>52</sub>	−6.44	6.8	7.3	4.3
C <sub>70</sub>	−6.57	C <sub>69</sub>	−6.46	7.3	6.6	7.1
C <sub>89</sub>	−6.64	C <sub>88</sub>	−6.55	7.3	7.3	7.1
C <sub>104</sub>	−6.74	C <sub>103</sub>	−6.66	7.7	8.9	8.6
C <sub>117</sub>	−6.80	C <sub>116</sub>	−6.73	8.0	7.6	8.6

**Table 2**

The difference in the DFT total energy of the  $C_{116}$  flake with vacancy in the middle and at the edge for a number of vacancy sites defined by the distance  $d$  (in Å) from the edge. The first row refers to the vacancy site shown in Figure 3.

Vacancy site	1	2	3	4	5	6	7	8	9
$\Delta E$	8.0	7.4	7.2	6.5	7.1	4.4	1.9	0.0	0.0
$d$	8.6	7.2	6.5	5.1	4.3	2.9	2.2	0.7	0.0

cancy site and prominent bending and distortion of the entire structure. Table 2 presents the difference in the total energy of the  $C_{116}$  flake with a vacancy in the middle and at the edge for a number of vacancy sites along its path towards the edge defined by the distance  $d$  shown in Figure 3. For distances of  $d \gtrsim 4 \text{ \AA}$  from the edge the vacancy adopts the 5/9 configuration (positions 1–5 in Figure 3). The decrease of  $\Delta E$  with decrease of the distance between the vacancy and the edge is monotonic for positions 1–4. This means that in small flakes directional motion of the vacancy towards the edge might be a thermodynamically driven process. Similar observation has been recently reported for small hydrogen terminated graphene flakes [15]. A small increase of  $\Delta E$  for vacancy transition from position 4 to 5 can be explained by the fact that this step does not correspond to the motion towards the nearest edge. The energy difference,  $\Delta E$ , between position 1 and position 4 is 1.5 eV, and it is mainly due to the decrease in distortion of the optimised structure of the flake as the vacancy moves closer to the edge.  $\Delta E$  between positions 4 and 9, however, is 6.5 eV, and it is related to the edge reconstruction leading to elimination of the dangling bond. Note that not only removal of carbon atom directly at the edge (positions 8 and 9) leads to the edge reconstruction, the next row of atoms (positions 6 and 7) also actively contribute to it. Thus only a small part of  $\Delta E$  (1.5 eV out of the total of 8.0 eV in the case of the  $C_{116}$  flake) can be related to the vacancy motion near the edge. However in a small graphene flake this is sufficient for directional motion of the vacancy towards the edge at room temperature.

For infinite graphene sheet with a single vacancy the 5/9 vacancy structure corresponds to the ground state having three possible equivalent configurations. These configurations are separated by a small barrier which was calculated [9] to be considerably smaller than the barrier to the vacancy transition to an adjacent 5/9 state, so that each of the three equivalent configurations is formed transiently. For infinite graphene, therefore, vacancy motion occurs through a single transition state between the adjacent 5/9 states [26]. For finite graphene, however, the ground state corresponds to the structure with vacancy at the edge, whereas the 5/9 and spiro vacancy configurations in the middle are metastable.

For the model  $C_{116}$  flake, the total DFT energies and structures of the metastable and transition states have been calculated along the vacancy path towards the edge. It has been found that vacancy transition between the adjacent 5/9 states near graphene edge can actually occur through one spiro state and two transition states. A general scheme which describes all possible transitions between the adjacent metastable states of vacancy in the middle of the  $C_{116}$  flake is shown in Figure 4a. The starting vacancy configuration is taken to be the 5/9 state shown in Figure 4a as 5/9A with its structure detailed in Figure 4b. In the 5/9A state the distance between two carbon atoms marked as A and B is 2.60 Å. The TSC transition state has been found in which the distance between atoms A and B is reduced to 2.15 Å (Figure 4c). The SB spiro state is formed as a result of bond formation between atoms A and B (Figure 4d). The obtained structure of the transition state is similar to that found for the hydrogen terminated graphene flakes [9,15] and

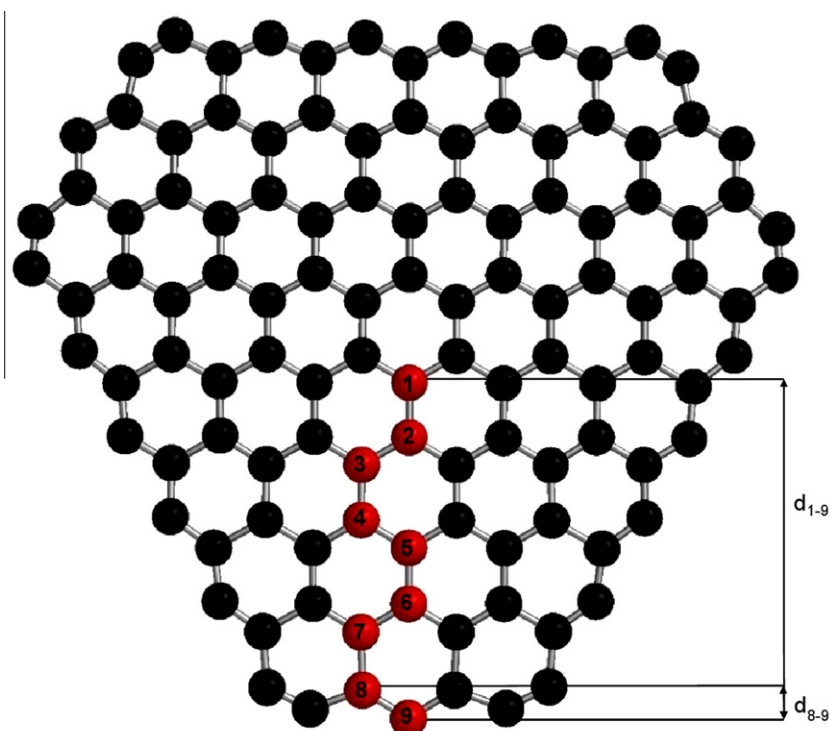


**Figure 3.** The model  $C_{116}$  flake showing vacancy site 1–9 in red, which refer to the first row in Table 2;  $d$  is the distance between the vacancy site inside the flake and at the edge. (For interpretation of the references to colour in this figure legend, the reader is referred to the web version of this article.)

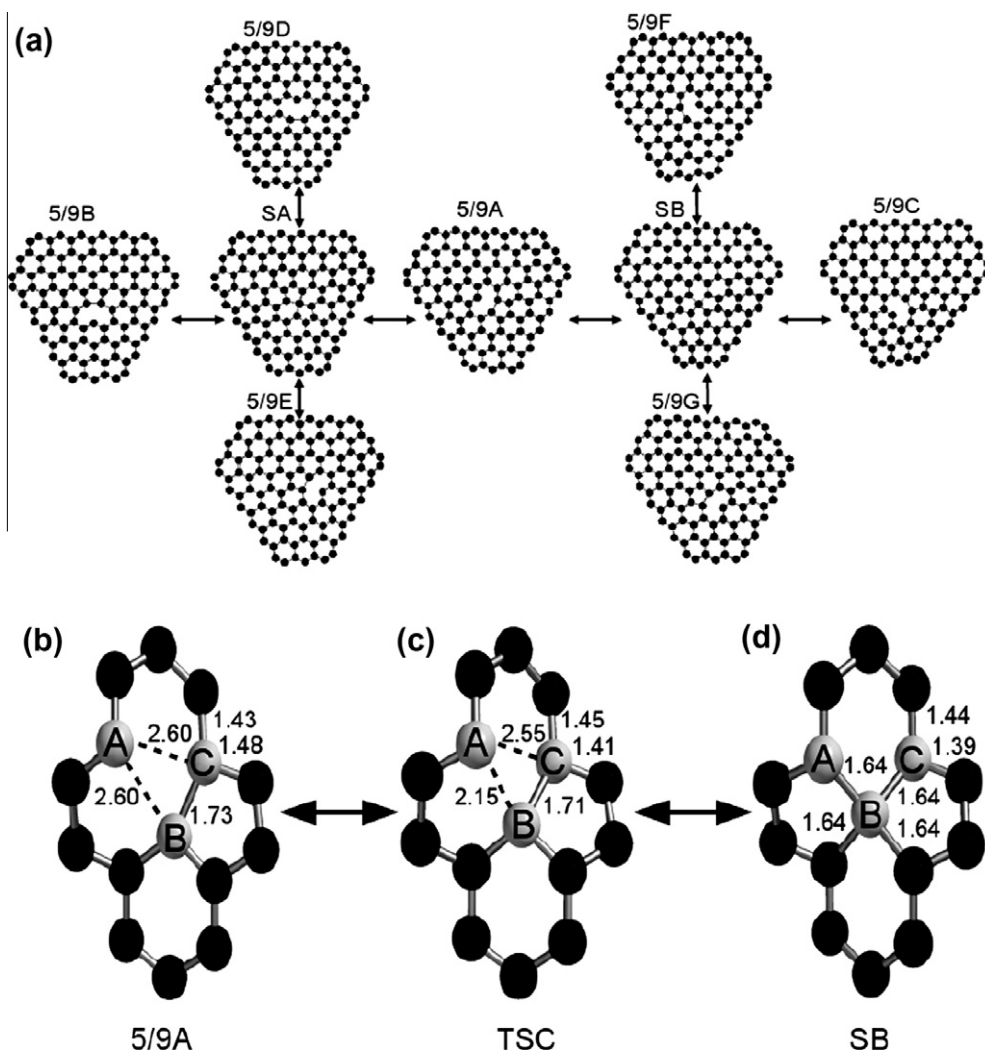


**Figure 4.** (a) Possible transitions between the neighbouring 5/9 vacancy states in the model  $C_{116}$  flake; (b–d) local structure of the vacancy: (b) the 5/9 state, (c) the transition state, (d) the spiro state.

infinite graphene [26]. A transition from the 5/9A state to another spiro state, marked as SA, is also possible, and this results in bond formation between atoms A and C. In the SB spiro state, atom B is bound to four carbon atoms with the bond length of 1.64 Å (as shown in Figure 4d). Thus transitions from the SA spiro state to the four possible 5/9 states – the initial 5/9A state and three new states 5/9B, 5/9D and 5/9E – can be achieved by breaking one of the four bonds. The 5/9B state corresponds to another configuration for the structure of vacancy created by removal of the same atom as in the case of the 5/9A state. The 5/9D and 5/9E states, however, correspond to a vacancy created by removal of a different atom in the flake, and therefore these states assume the motion of vacancy. A similar process takes place for transitions from the SB spiro state to the 5/9 states marked as 5/9C, 5/9F and 5/9G in Figure 4a. The 5/9F state correspond to the last of the three configurations of the initial vacancy structure, and the 5/9C and 5/9G states describe the vacancy motion.

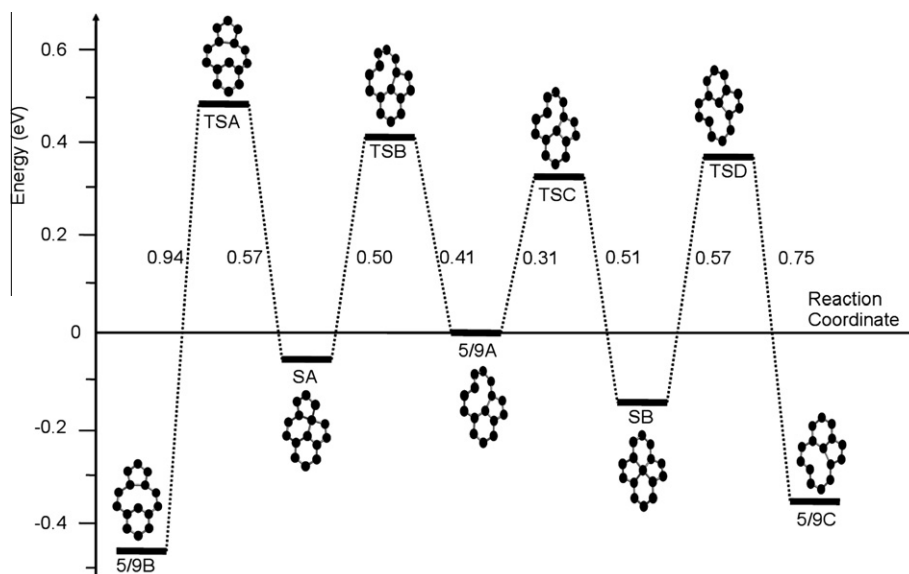
The reaction path connecting the 5/9B and 5/9C states is shown in Figure 5. Two cases are considered: (1) transition of the vacancy between configurations 5/9A and 5/9B, which are created by removal of the same atom; (2) transition between two different configurations 5/9A and 5/9C created by removal of adjacent atoms. Unlike the case of infinite graphene, three configurations obtained by removal of one atom from a small finite flake are not equivalent due to the flake distortion specific to each configuration. Indeed,

Figure 5 shows that the total energy of the  $C_{116}$  flake with vacancy in 5/9B and 5/9A configurations differs by about 0.43 eV. For the considered example, the barrier to the transition between different configurations of the same vacancy is slightly higher than that to the vacancy motion. This result is somewhat different to the conclusions made for infinite graphene [9], and it emphasizes the difference in dynamic behaviour of the vacancy near graphene edge and far from it. The obtained barriers for vacancy motion near the edge are smaller than the values of 1.6 eV [11], 1.3/1.4 eV [26], and 1.37 eV [13] predicted for infinite graphene. Our values, however, are in good agreement with the barrier to vacancy motion towards the neighbouring vacancy separated by two hexagonal rings, which is predicted to be 0.94/1.01 eV [12]. Thus a conclusion can be made that the barrier to vacancy motion tends to decrease with decrease of the distance between the vacancy and graphene edge.

The average time,  $t_s$ , necessary for the vacancy to change position is determined by Arrhenius formula:

$$t_s = \frac{1}{\nu} \exp\left(\frac{E_a}{kT}\right), \quad (3)$$

where the value of  $\nu$  has the same order of magnitude as the frequency of atom vibrations in the lattice, and  $E_a$  is the highest activation energy along the reaction path. For the reaction path



**Figure 5.** For the model  $C_{116}$  flake, the DFT total energy change as a function of reaction coordinate for vacancy transition between the neighbouring 5/9 vacancy states; the energies are presented relative to the energy of the 5/9A state. The differences in the total energy between the transition states and the local minima corresponding to the 5/9 and spiro states are presented. The local structure of vacancy for the considered states is also shown.

between the states 5/9A and 5/9C the highest activation energy for the motion towards the edge is 0.57 eV, and this value is 0.75 eV for the vacancy motion away from the edge (Figure 5). Taking  $v$  to have the value of  $10^{13} \text{ s}^{-1}$  the average time at room temperature is estimated to be  $t_s = 4 \times 10^{-4} \text{ s}$  for the motion towards the edge, and  $t_s = 0.4 \text{ s}$  for the motion away from the edge. For the considered step of vacancy motion, the probability of a move towards the edge is three orders of magnitude greater than the probability of a move away from the edge. Therefore, the vacancy near the edge will undergo the directional motion towards the edge.

To support this conclusion the MD simulations of vacancy motion near graphene edge have been performed. The difference in the total energy of the  $C_{116}$  flake with vacancy at different locations in the flake (shown in Figure 3) obtained using the Brenner potential has similar trend to that predicted by DFT and shown in Table 2. For example, the energy difference between the flake with vacancy in position 1 and position 4 is predicted to be 0.6 eV using the Brenner potential (this value can be compared to the DFT value of 0.9 eV). This is not surprising as the Brenner potential [24] has been specifically parametrized to fit the energetics of the individual C–C and C–H bonds within the hydrocarbons. Therefore, despite the *ad hoc* nature of the extra terms in the Brenner potential it is adequate for qualitative study of the dynamic behaviour of vacancy near graphene edge. The calculated values for the total average time  $\langle t \rangle$  that takes for a vacancy in the flakes shown in Figure 2 to reach the edge are presented in Table 3 for hexagonal shapes (Figure 2a–d) and in Table 4 for short rectangular flakes (Figure 2e–g). In the case of vacancy diffusion the average time  $\langle t \rangle$  is proportional to the squared distance  $d^2$  between the initial position of vacancy and the edge. However the results presented in Tables 3 and 4 show considerably slower increase in the average time  $\langle t \rangle$  with the distance  $d$ , which implies directional motion of the vacancy towards the edge rather than its diffusion. This conclusion is also confirmed by a direct analysis of trajectories of moving vacancies. For the smaller flakes,  $C_{116}$ ,  $C_{176}$  and  $C_{248}$ , the directional motion of the vacancy towards the edge has been clearly observed. An example of the vacancy trajectory directly towards the edge is shown in Figure 6a. For greater flakes,  $C_{332}$ ,  $C_{395}$ ,  $C_{447}$  and  $C_{623}$ , diffusion of vacancy located far from the edge has been also noticed. An example of the trajectory in which diffusion of vacancy takes

**Table 3**

The MD average time  $\langle t \rangle$  (in ps) for vacancy motion from the middle to the edge of hexagonal flakes;  $d_{\min}$  and  $d_{\max}$  (in Å) are the shortest and the longest distances, respectively, between the initial position of vacancy and the edges. At least 20 runs have been produced for each flake.

Flake	$d_{\min}$	$d_{\max}$	$\langle t \rangle$
$C_{116}$	7.0	9.9	$260 \pm 5$
$C_{176}$	8.4	12.7	$490 \pm 5$
$C_{248}$	11.3	14.5	$560 \pm 10$
$C_{332}$	12.7	16.9	$610 \pm 15$

**Table 4**

The MD average time  $\langle t \rangle$  (in ps) for vacancy motion from the middle to the edge of rectangular flakes and nanoribbon;  $d_a$  and  $d_z$  (in Å) are the distances between the initial position of vacancy and the armchair and zigzag edges, respectively. At least 20 runs have been produced for each flake and 60 for nanoribbons.

Flake	$d_z$	$d_a$	$\langle t \rangle$
$C_{395}$	15.5	14.7	$760 \pm 8$
$C_{426}$	15.5	18.7	$900 \pm 10$
$C_{623}$	15.5	23.3	$880 \pm 10$
Nanoribbon	15.5	–	$1150 \pm 10$

place before the directional motion towards the edge takes over is shown in Figure 6b. Diffusion of vacancy occurs at the distance from the edge that exceeds  $d \approx 10 \text{ Å}$ , whereas the directional motion towards the edge takes over at the distances less than  $10 \text{ Å}$ . Once the vacancy reaches the edge it remains at the edge for the entire duration of simulation lasting 2 ns. The motion of the vacancy along the edge has been also observed in a number of simulation runs. For all considered flakes vacancy moves more often to the closest edge showing no preference to armchair or zigzag edges.

The motion of vacancy in infinite zigzag-edged graphene nanoribbons has been also simulated in periodic boundary conditions. The width of the infinite nanoribbon was taken to be  $31 \text{ Å}$ , the same as the distance between zigzag edges of rectangular flakes shown in Figure 2e–g. The initial distance  $d_z = 15.5 \text{ Å}$  between the vacancy and zigzag edge also agrees with the value of  $d_z$  in short rectangular flakes (Table 4). The average time  $\langle t \rangle$  for the

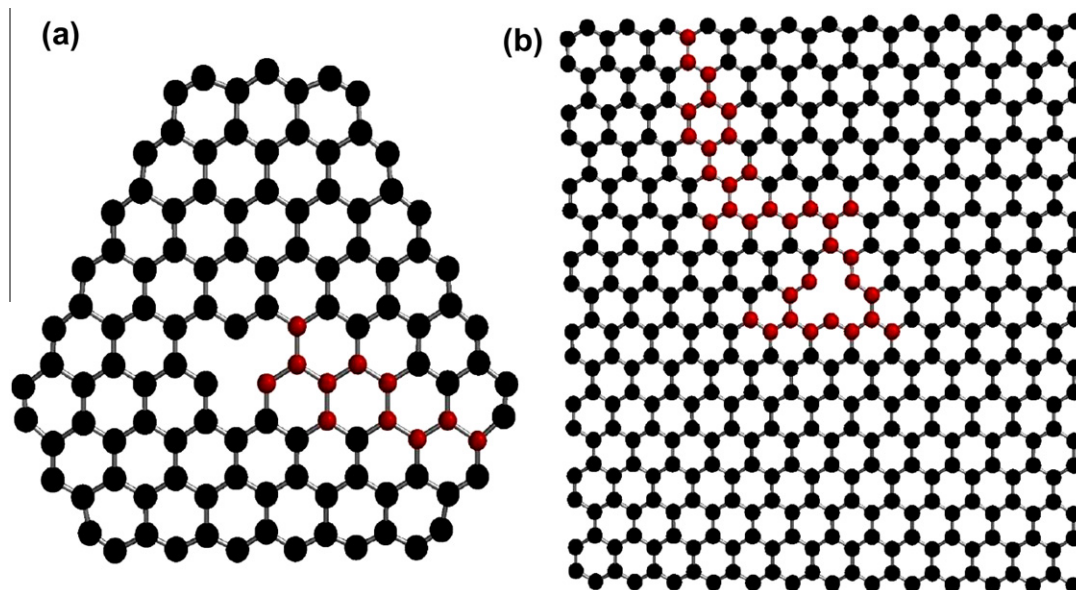


**Figure 6.** Examples of the MD trajectories (shown in red) for the vacancy motion: (a) in the  $C_{116}$  hexagonal flake, (b) in the  $C_{395}$  rectangular flake. (For interpretation of the references to colour in this figure legend, the reader is referred to the web version of this article.)

motion of vacancy to the zigzag edge in the infinite length nanoribbon is obtained to be 1150 ps, this value is greater than those predicted for the finite rectangular flakes of the same width. For 9 out of 60 runs performed with duration of 2 ns, vacancy does not reach the edge. These simulation results show the diffusive character of vacancy motion in the middle of the nanoribbon.

The presented calculations underpin the mechanisms driving structural transformations in graphene, which have been observed recently in AC-TEM experiments [7,29]. Self-healing of a hole in graphene layer has been reported in TEM experiments at  $T = 600$  K [29], which occurs due to its filling by carbon ad-atoms removed by the imaging electron beam from graphene edge. Our MD simulations show that the motion of vacancy towards the edge has diffusive character in flakes and nanoribbons with dimensions greater than 20 Å. The DFT value of 1.37 eV [13] for the barrier to vacancy diffusion in infinite graphene is relatively small. Therefore, motion of vacancies to the edge due to diffusion can also take place in larger extended layers. Similarly the self-healing mechanism discussed in [29], self-healing due to diffusion to the edge will be more efficient at higher temperatures. It has to be noted that the phonon thermal conductance of nano-graphene sheets is greatly affected by the presence of a vacancy defect [30]. A divacancy defect, formed by removal of carbon atom adjacent to a vacancy or due to coalescence of two monovacancies, has a barrier to diffusion as large as 7.5 eV [13]. This defect cannot diffuse to the edge, and it acts as an origin of a hole formation since it can also attract monovacancies similar to the edge. To prevent the formation of divacancies the concentration of monovacancies needs to be sufficiently small. The concentration of vacancies in graphene is determined by the competition between two processes: ejection of carbon atoms due to radiation damage (for example, a knock-on collision with electron of the imaging beam) and diffusion of vacancies towards the edge where they are finally caught. If the rate of vacancy formation is considerably less than the rate of diffusion to the edge than the concentration of monovacancies remains small, and the probability of formation of divacancy defects is negligible. In this case radiation damage occurs only at the edge, and the size of the finite flake decreases keeping the structure defect-free in the middle. The diffusion of vacancy along the graphene edge observed in MD simulations can also contribute to self-healing of graphene edge, which will affect the electronic properties of graphene nano-

ribbons. This makes graphene flakes and nanoribbons attractive for applications in nanoelectronic devices resistant to radiation damage, for example, in space satellites.

In the proposed 'top-down' mechanism for fullerene formation directly from a flat graphene flake in AC-TEM [7], the initial size of the graphene flake is important as it determines the size of the formed fullerene cage. In large extended flakes the van der Waals interaction between the substrate and the flake prevents the structure transformation. The edges of large flakes continue to be etched by the electron beam until the flake reaches an optimal size of about 150–300 atoms enabling the thermodynamically driven closure of fullerene cage. The calculations presented in this Letter show that if vacancy is created in the middle of such small flake by the imaging electron beam it has sufficient time to move to the edge even at room temperature. The probability that the vacancy returns back inside the flake is negligible.

#### 4. Conclusions

The density functional theory within unrestricted Kohn–Sham approach has been used to calculate the total energies and structures of small graphene flakes ranging from  $C_{53}$  to  $C_{116}$  with the vacancies in the middle and at the edge. For all considered flakes, the position of vacancy at the edge was found to be energetically more favourable by 6.6–8.9 eV compared to vacancy in the middle. The energy difference between the two positions decreases with decrease of the flake size. For the model  $C_{116}$  flake the total energy has been calculated for a number of vacancy positions between the middle and the edge. It has been shown that the main part of the energy difference between the structure with vacancy inside the flake and at the edge is related to the edge reconstruction, whereas a small portion of about 1.5 eV is due to distortion of the flake structure.

The reaction path between two adjacent 5/9 vacancy states, corresponding to one step of the vacancy motion from the middle to the edge as well as transitions between different configurations of the same vacancy have been studied in detail. The reaction paths between two adjacent 5/9 states have been found to have similar activation energy and to occur through two transition states and a spiro metastable state. The highest activation energy along the

reaction path is calculated to be 0.57 eV for the motion of vacancy towards the edge and 0.75 eV for its motion away from the edge. The average time that one step of the vacancy motion takes at room temperature is estimated to be  $4 \times 10^{-4}$  s and 0.4 s for the motion towards the edge and away, respectively. This implies that for graphene-like structures with dimensions within 20 Å studied in AC-TEM, vacancy has sufficient time to move to the edge between the subsequent electron knock-on events even at room temperature. At the same time, the probability for the vacancy to leave the edge is negligible.

The dynamic behaviour of vacancy near graphene edge has been studied using MD simulations. The analysis of the calculated average time of vacancy motion towards the edge and vacancy trajectories reveals that the dynamics depends on the distance between the vacancy and the edge. The vacancy moves directly towards the nearest edge if the distance is less than 10 Å, otherwise a random diffusion takes place. Thus the interactions between the electron of the imaging beam and vacancy located near the edge can be excluded from the analysis of mechanisms driving structural transformations of graphene-like systems in AC-TEM. The obtained results also show that vacancy diffusion plays important role in graphene self-healing.

#### Acknowledgements

E.B. acknowledges EPSRC Career Acceleration Fellowship and New Directions for EPSRC Research Leaders Award (EP/G005060). A.P. acknowledges Russian Foundation of Basic Research (Grant 1202-90041-Bel and 11-02-00604-a) and Samsung Global Research Outreach Program.

#### References

- [1] J.C. Meyer, C. Kisielowski, R. Erni, M.D. Rossell, M.F. Crommie, A. Zettl, *Nano Lett.* 8 (2008) 3582.
- [2] C.O. Girit et al., *Science* 323 (2009) 1705.
- [3] J.H. Warner et al., *Nat. Nanotech.* 4 (2009) 500.
- [4] A. Chuvilin et al., *Nat. Mat.* 10 (2011) 687.
- [5] A.V. Talyzin et al., *Nano Lett.* 11 (2011) 4352.
- [6] T.W. Chamberlain et al., *Nat. Chem.* 3 (2011) 372.
- [7] A. Chuvilin, U. Kaiser, E. Bichoutskaia, N.A. Besley, A.N. Khlobystov, *Nat. Chem.* 2 (2010) 450.
- [8] A. Hashimoto, K. Suenaga, A. Gloter, K. Urita, S. Iijima, *Nature (Lond.)* 430 (2004) 870.
- [9] A.A. El-Barbary, R.H. Telling, C.P. Ewels, M.I. Heggie, P.R. Briddon, *Phys. Rev. B* 68 (2003) 144107.
- [10] J.M. Carlsson, M. Scheffler, *Phys. Rev. Lett.* 96 (2006) 046806.
- [11] E. Kaxiras, K.C. Pandey, *Phys. Rev. Lett.* 61 (1998) 2693.
- [12] G.D. Lee, C.Z. Wang, E. Yoon, N.M. Hwang, D.Y. Kim, K.M. Ho, *Phys. Rev. Lett.* 95 (2005) 205501.
- [13] H. Zhang, M. Zhao, X. Yang, H. Xia, X. Liu, Y. Xia, *Diamond Relat. Mater.* 19 (2010) 1240.
- [14] M.W.C. Dharma-Wardana, M.Z. Zgierski, *Physica E* 41 (2008) 80.
- [15] G. Xingfa, L. Lili, S. Irle, S. Nagase, *Angew. Chem. Int. Ed.* 49 (2010) 3200.
- [16] S. Banerjee, D. Bhattacharyya, *Comp. Mat. Sci.* 44 (2008) 41.
- [17] J.A. Pople, P.M.W. Gill, N.C. Handy, *Int. J. Quantum Chem.* 56 (1995) 303.
- [18] A.D. Becke, *J. Chem. Phys.* 98 (1992) 5648.
- [19] J. Kong et al., *J. Comput. Chem.* 21 (2000) 1532.
- [20] X. Gao, L. Liu, S. Irle, S. Nagase, *Angew. Chem. Int. Ed.* 49 (2010) 3200.
- [21] O.V. Yazev, *Phys. Rev. Lett.* 101 (2008) 037203.
- [22] H. Tachikawa, H. Kawabata, *J. Phys. Chem. C* 113 (2009) 7603.
- [23] J.D. Gale, A.L. Rohl, *Mol. Stimul.* 29 (2003) 291.
- [24] J.W. Brenner, *Phys. Rev. B* 42 (1990) 9458.
- [25] I.V. Lebedeva, A.A. Knizhnik, A.M. Popov, B.V. Potapkin, *J. Phys. Chem. C* 116 (2012) 6572.
- [26] A.V. Krashennnikov, P.O. Lehtinen, A.S. Foster, R.M. Nieminen, *Chem. Phys. Lett.* 418 (2006) 132.
- [27] P.A. Throver, R.M. Mayer, *Phys. Status Solidi A* 47 (1978) 11.
- [28] M.T. Luck, L.D. Carr, *Phys. Rev. Lett.* 100 (2008) 175503.
- [29] B. Song, G.F. Schneider, Q. Xu, G. Pandraud, C. Dekker, H. Zandbergen, *Nano Lett.* 11 (2011) 2247.
- [30] J.-W. Jiang, B.-S. Wang, J.-S. Wang, *Appl. Phys. Lett.* 98 (2011) 113114.